SAKARYA ÜNİVERSİTESİ
FEN BİLİMLERİ ENSTİTÜSÜ DERGİSİ

Sakarya University Journal of Science
SAUJS

e-ISSN 2147-835X Founded 1997 Period Bimonthly Publisher Sakarya University
http://www.saujs.sakarya.edu.tr/en/

Title: Electromagnetic Shielding Properties of Pack Borided MirraxTM Steel

Authors: İbrahim ALTINSOY

Recieved: 2021-01-14 00:00:00

Accepted: 2021-10-13 00:00:00

Article Type: Research Article

Volume: 25
Issue: 6
Month: December
Year: 2021
Pages: 1304-1312

How to cite
İbrahim ALTINSOY; (2021), Electromagnetic Shielding Properties of Pack Borided MirraxTM Steel. Sakarya University Journal of Science, 25(6), 1304-1312, DOI: https://doi.org/10.16984/saufenbilder.860759
Access link
http://www.saujs.sakarya.edu.tr/tr/pub/issue/66341/860759

Sakarya University Journal of Science 25(6), 1304-1312, 2021

Electromagnetic Shielding Properties of Pack Borided Mirrax™ Steel

İbrahim ALTINSOY*[1]

Abstract

In this study, it was aimed to investigate the electromagnetic interference shielding (EMI-SE) as well as some physical and mechanical properties of pack borided Mirrax tool steel. Boriding process was carried out at 900, 950 and 1000°C for 2, 5, 8h, respectively. Optical images showed that borides layer have smooth morphology and flat interface with matrix. XRD analysis revealed that main phases in the layer were FeB and Fe_2B. Intensity of FeB phases increased with increment of process temperature and time. Depending on process time and temperature, the thickness of borides layer was ranged from 10 µm to 87.80 µm. Microhardness of layer was between 1700 and 2400 HV. EMI-SE measurements conducted within Ku band (12-20 GHz) indicated that EMI-SE efficiency increased by increasing of process time and temperature and it was ranged from 52dB to 75dB. It is possible to claim that borided Mirrax steel performed good EMI-SE and when boriding time reached to 5h, remarkable EMI-SE (electromagnetic interference shielding) (over 60dB) was observed on the samples borided at 900°C.

Keywords: pack boriding, borides, EMI-SE, microhardness, layer thickness.

1. INTRODUCTION

The rapid proliferation of diverse electro/electrical products and technology has resulted in the increase of electromagnetic pollution known as electromagnetic interference (EMI) to greater levels. This ever-increasing electromagnetic pollution can produce severe interference effects and may cause detrimental effects on device performance and human health [1, 2]. Therefore, the issues caused by electromagnetic interference are exposed to people accompanied by the transmission of high-energy electromagnetic radiation, and have become critical problems needed to be addressed. Electromagnetic interference (EMI) and electromagnetic wave pollution will not only cause interference and serious impact on electronic equipment, but also cause harm to human health. Also, in national defense and military fields, electromagnetic wave leakage will seriously harm national defense information security and state secret protection [2, 3]. EMI can be shielded by mechanisms involving reflection and absorption of electromagnetic (EM) radiation. Reflection occurs through interactions of incident EM waves with mobile charge carriers (electrons or holes) of an electrically conductive material [2]. To minimize these issues arising due to EMI, effective shielding materials are in need to protect the efficient operation of electro/electrical systems. And they are widely employed to prolong the service life of equipment, improve the electromagnetic

* Corresponding author: ialtinsoy@sakarya.edu.tr
[1] Sakarya University, Engineering Faculty, Department of Metallurgy and Materials Engineering, Turkey.
ORCID: https://orcid.org/0000-0003-4284-5397

compatibility (EMC) and security of biological systems, whilst reduce the impact and harm in electromagnetic radiation on the human body or the equipment being interfered [1,3]. As a result, searching for high performance EMI shielding materials has become a burgeoning field of research. Currently, the most commonly used materials for EMI shielding are metals, such as stainless steel, copper, aluminum, silver, etc. due to good electrical conductivity, metals exhibit excellent EMI shielding performance. However, many metals come across problems of high specific weight, susceptibility to corrosion, and easy oxidation [4]. Among these materials, the diffusion of hydrogen into steels results in a number of problems such as; hydrogen-induced cracking, hydrogen stress cracking, sulfide stress corrosion cracking and hydrogen embrittlement [5]. With the increasing demand for EMI shielding in various applications, such as high temperature and corrosion circumstances, as well as hydrogen infiltration, there exists a growing interest in exploring suitable materials [4]. For this purpose, boriding of steel substrates should be promising approach and there is limited reports in open literature about EMI shielding effectiveness of borided steels.

Boriding, being a kind of thermo-chemical surface hardening process by which boron is introduced onto the surface of the steels and its alloys at elevated temperature and generally applied to engineering components to increase the superficial hardness, enhance their oxidation, abrasion, and erosion resistance [6,7, 8]. The formation borides such as FeB and Fe_2B depends on the process temperature, the chemical composition of the substrate steel, the boron potential of the medium and the duration of the boriding [9, 10]. The material alloy composition also plays an important role in the morphology and properties of the boride layer [10]. Borided surfaces can maintain their hardness, wear properties up to 1000 °C. One of the most important features of the borided surface is to retain its hardness even after additional heat treatment [11]. Various boriding techniques such as powder-pack boriding, liquid boriding, plasma boriding and gas boriding have been developed [12,13]. Pack boriding method is frequently used because of having technical favors and cost efficiency [11, 12]. The process consists of packing the samples in a powder mixture rich in boron inside of a stainless steel box [14]. Ferrous and non-ferrous materials are commonly borided in temperature range of 850–1000 °C and with treatment time range of 1–10 h or more in pack boriding process [11].

The aim of this study, to enhance surface properties such as ~~high~~ increasing hardness of Mirrax tool steel, by pack boriding method and investigate EMI shielding properties of the borided surface formed on the studied steel sample within the Ku band range. The main driving force of this report is there are limited reports about EMI-SE effectiveness of borided steels in open literature and therefore, it was focused on EMI-SE tests as well as the mechanical , morphological properties of borides formed on the Mirrax steel surface.

2. MATERIALS and METHOD

Mirrax steel samples with dimensions of 20x15x10 mm were ground with 240,320, 400 and 600 number SiC papers and at each grinding stage, grinding papers were lubricated with stream of water. Then, all samples were washed and dried. After drying, samples were taken to polishing wheel and polished with 1 μm diamond past in order to clean surface and enhance the boron diffusion efficiency prior to boriding process. Pack boriding was realized at 900, 950, 1000°C for 2, 5, 8h, respectively by sealing samples within steel container with Ekabor® as boronizing source and Ekrit® powders, for preventing possible oxidation. Chemical properties of the Mirrax steel was given in Table 1.

After boronizing, samples were grinded with SiC abrasive paper up to1000 grid and then polished with 1 μm alumina suspension. Polished samples were etched with 3 % of Nital (vol. 3% HNO_3-vol. 97%Ethanol) in order to carried out optical microscopy observation. The borides layer formed on the surface of steel substrate were examined via Nikon Eclipse L200 optical microscope. Layer thickness was measured with

image analysis from the optical micrographs as-taken. XRD analysis was conducted by Rigaku PC2200 using CuKα with a wavelength of 1.54 nm between 20-90° range in order to detect boride phases in the borided layer. Microhardness of borides and variation of hardness from borides to matrix were measured by Nikon VM-HTMod with a load of 50g. Electromagnetic Interference Shielding test was carried out via Vector Network Analyzer (Agilent ENA E5071C) according to ASTM D4935 within the Ku band (12-20 GHz). Thickness of borided samples was reduced to 2 mm in order to elude the shielding efficiency of metallic matrix before EMI-SE test.

Table 1 Chemical composition of Mirrax® Steel

Elements/Chemical Composition, wt.%						
C	**Si**	**Mn**	**Cr**	**Mo**	**Ni**	**V**
0.25	0.35	0.55	13.3	0.35	1.35	0.35

3. RESULTS AND DISCUSSIONS

3.1. Optical Microstructure

Optical images of Mirrax sample borided at 900-1000°C for 2-8h were illustrated in Figure 1-3 (a-c). As it can be seen from optical micrographs, borided layer had smooth morphology and flat interface between layer and matrix. It was resulted from alloying elements of Cr, Ni due to high amount of Cr and Ni in the Mirrax steel matrix restricted the growing of borides layer [9, 15, 16, 17]. These elements, especially Cr, also has higher dissolution ability in the layer according to iron matrix because of atomic number of Cr was lower than that of Fe and therefore, higher porosity can be seen towards surface of the borides layer. It was probably resulted from more Cr promoted towards the surface of the borides layer by boriding temperature and time increased (Fig.1-3 a-c)[15]. On the other hand, Ni tends to accumulate at the end of borides layer during boriding process [16] and it can be claimed that grayish-black coloured zone beneath the layer indicated Ni and also Cr rich region. Ni elements pushed towards the tips of borides also formed the complex (Fe,Ni)B [16] as well as some Cr-borides with grayish-green coloured particle morphology at the grain boundaries and some of them can take place in the steel matrix observed as grayish-green colored small bright particles (Fig. 2-3b-c). As boronizing time and temperature progress, the borides layer became more porous as more alloying elements take place of iron during boriding and it leaded to more porosity formation [16].

It can be seen from optical micrographs, borided layer thickness increased with decreased growing rate by boriding progress and temperature raised (Fig. 1-3a-c). This is well-known diffusion phenomenon and in the presence of high alloying elements (Cr), growing of the borides layer become difficult. The nature of borides layer had polyphase morphology and consisted of FeB/Fe_2B (Fig. 2b). This polyphase nature was obviously seen in the samples borided at 950 and 1000 °C. At the beginning of the boriding process, boron diffusing occurs first, and Fe_2B phase is formed by the reaction of boron with iron. By increasing the thickness of this boride layer, the boron diffusion towards the end of borides and matrix is reduced and the FeB phase, which has higher boron content, starts to form on the Fe_2B phase by reaction of B with outer section Fe_2B (Fig. 2-3a-c) [9, 18].

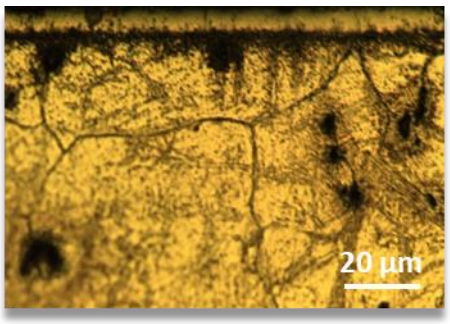

a)

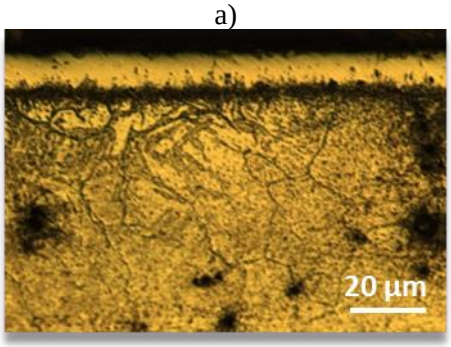

b)

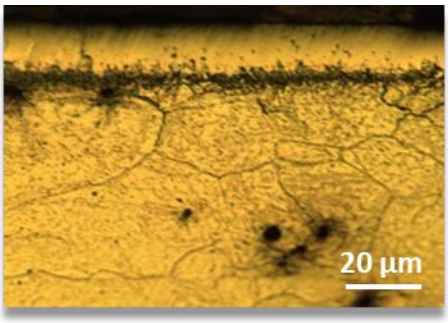

c)

Figure 1 Optical micrographs of Mirrax steel borided at 900°C, **a)** 2h, **b)** 5h, **c)** 8h.

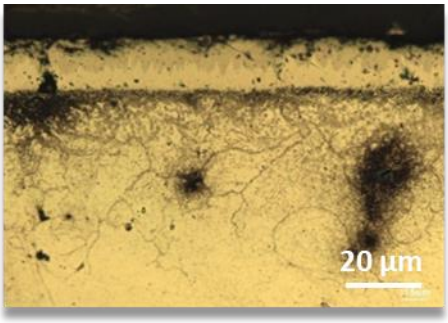

a)

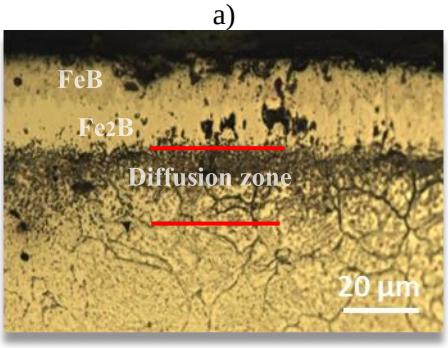

b)

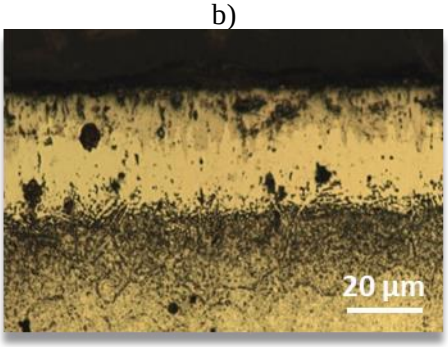

c)

Figure 2 Optical micrographs of Mirrax steel borided at 950°C, **a)** 2h, **b)** 5h, **c)** 8h.

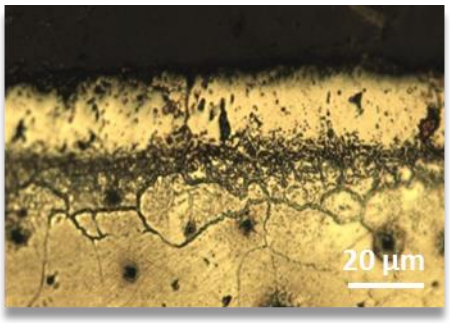

a)

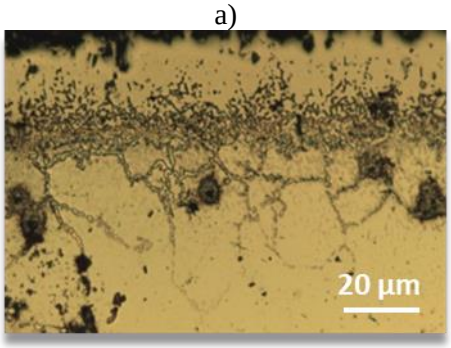

b)

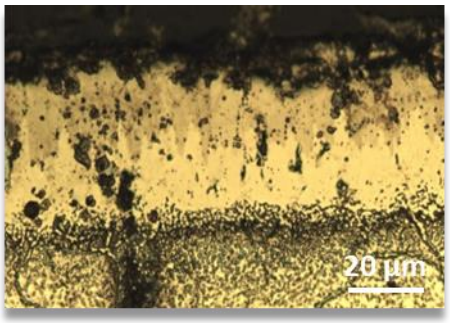

c)

Figure 3 Optical micrographs of Mirrax steel borided at 1000°C, a) 2h, b) 5h, c) 8h.

3.2. Layer Thickness

Variation of borides layer thickness was presented in Table 2 and it can be seen from Table 2, when boriding temperature increased, the thickness of borides layer rapidly growth for the short process time, 2h. So that, four time higher thickness for sample borided at 1000°C, 2h was measured compared to that of sample borided 900°C, 2h and the growing rate of borides reduced from four times to three and two-half times in the samples borided for 5 and 8h, respectively by increasing temperature. The growing of layer got slower when the process time increased for increasing temperatures. On the other hand, boriding temperatures was more dominant factor for growth of the borides layer. The obtained

results was coming from nature of diffusion phenomenon as boronizing is diffusion base process, and results were similar to reports related to boriding of AISI 420 steel [16, 19]. Mirrax steel was derivated and developed from AISI 420 steel, thus similar but lower layer thickness was measured in Mirrax steel than that of AISI 420 due to higher amount of Cr and Ni according to AISI 420 steel.

Table 2 Borides Layer thickness depending on boriding time and temperature

Boriding Time (h)	Boride Layer Thickness (µm)		
	Boriding Tempereature (°C)		
	900	950	1000
2	11,55	32,06	43,85
5	21,32	46,50	66,63
8	33,51	62,20	86,15

3.3. XRD Analysis

XRD analysis of the boride samples were shown in Figure 4a-c.

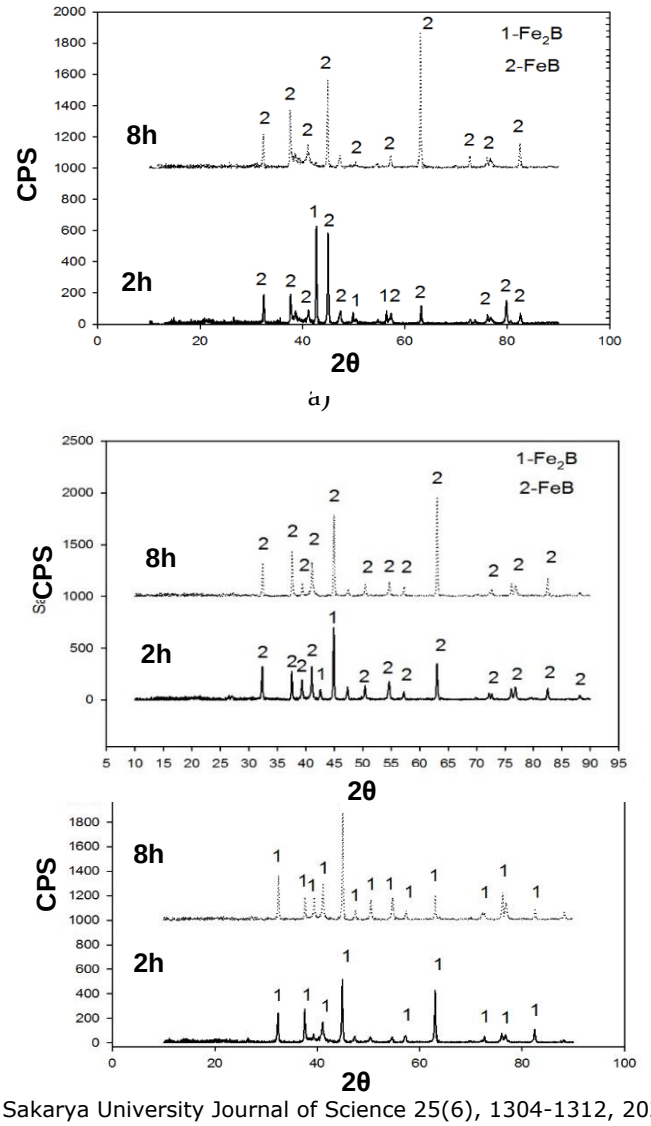

Figure 4 XRD analysis of borided Mirrax Steels according to boriding temperature, a) 900°C, b) 950°C, c) 1000°C.

When boriding process have just started, Fe_2B initially formed followed by saturation of matrix with boron. As boronizing process progressed, Fe_2B layer growth restrictly due to high amount of Cr as well as some Ni in the steel matrix and FeB started to form by reaction of boron rich Fe_2B on outer side of Fe_2B phase. Therefore, remarkable amount of FeB was detected in the sample even borided at 900°C for 2h (Fig. 4a). According to XRD analysis, FeB formation accelerated with increasing temperature and time. for 8h This led to detection of only FeB on the surface of borided matrix as thickness of FeB layer which took place outer zone of the borides increased with increment in boronizing time and tempearature. (Fig. 4b-c). It was reported that double phase (FeB/Fe_2B) was common for high alloy steels. [14, 17] Althogh there was high amount of Cr in the samples, there was no CrB detected due to possible a relative low intensity and a low volume fraction of the chromium boride phases within the borides layer [17].

3.4. Microhardness

Microhardness of borides formed on the steel samples was ranged from 1672 HV to 2215 HV by increasing of boriding temperature and times. Microhardness of the borided samples was four times higher than that of Mirrax steel matrix (500HV) which was higher than that of annealed Mirrax steel (250 HV) [20] (Fig. 5a-c). It was reported that AISI 420 steel could be air quenched and hardness of air quenched AISI 420 steel was approximately 500 HV. Mirrax have similar heat treatment characterizations with AISI 420 steel and identical results obtained for Mirrax steel [20, 21]. During boriding process, steel matrix was possibly exposed to air quenching and that matrix hardness was measured.

It can be observed from the Figure 5a-c, penetration of high hardness continued towards more inner section of matrix due to increasing of borides layer consisting of FeB and Fe_2B with increment in the process time and temperature. It can be said that microhardness of over 1800 HV

was measured in max. 20 µm range in the samples borided at 900°C for 8h. There was also limited Ni rich diffusion zone having 600-1000HV microhardness observed in the same borided samples.

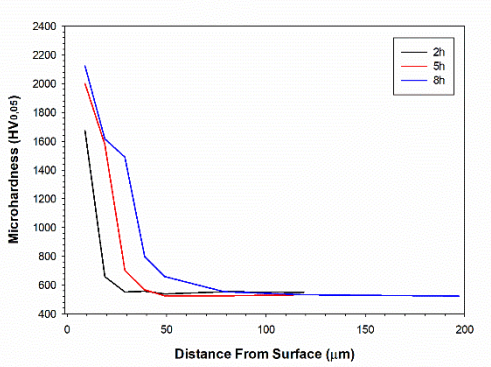

a)

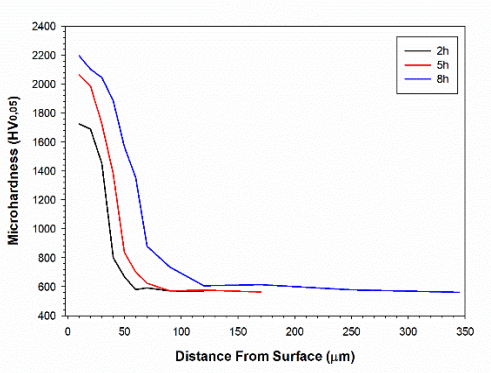

b)

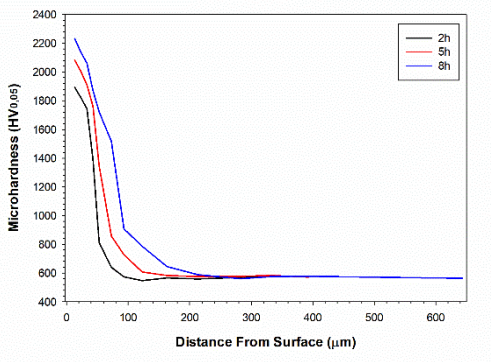

c)

Figure 5 Variation of microhardness from surface to interior of sample in the samples borided at a) 900°C, b) 950°C, c) 1000°C.

When boriding temperature raised to 950°C, it was observed that high microhardness of over 1800 HV could be measured up to 50 µm distance from the borides surface. Same phenomenon was seen up to 60 µm in the samples borided at maximum temperature. This was resulted from growing of the layer having FeB phase which is harder. By increasing of layer thickness, microhardness of 1800 HV was measured up to 75 µm, and diffusion zone also enlarged by increment in temperature and times. Microhardness of over 2000 HV measured in the all samples, except that of borided at 900°C for 2h possibly due to complex borides (Fe,Cr)B formation which was resulted from high amount of Cr within the FeB layer formed on the near surface regions (Fig.5a-c).

3.5. EMI-SE Analysis

EMI-SE (total) measurement were carried out within Ku band and results were presented in Figure 6a-c. Also, variation of mean EMI-SE with layer thickness was shown in Figure 7. As Figure 6a was investigated, it was found that at lower boriding temperature maximum EMI-SE was ranged from 60 to 74 dB by increasing process time. As boronizing time raised, variation of EMI-SE within Ku band seen in a narrower range. When boriding temperature increased to 950°C, maximum EMI-SE was measured between 70-79 dB. On the other hand, EMI-SE of sample borided at 950°C for 2h was significantly decreased to 60 dB after 13 GHz band passed and remained within 60-65 dB range up to 20 GHz. However, samples borided at 950°C for 5 and 8h performed higher EMI-SE efficiency and become more stable within the Ku band range. Samples borided at 1000°C had narrower, higher and more stable EMI-SE efficiency in the same band range. Maximum EMI-SE was ranged between 74 and 80 dB and samples caused a lower EMI-SE lost as boronizing time progressed with increased the band frequency (Fig. 6b-c).

When the layer thickness-EMI-SE relationship was examined, mean EMI-SE values reached the desirable maximum, 75 dB, at 46 µm borides layer thickness. After reaching out certain layer thickness, mean EMI-SE was not remarkably changed up to maximum layer thickness of 86 µm which belonged to sample borided at 1000°C for 8h (Fig. 7). It can be claimed that mean EMI-SE was increased by increasing of layer thickness up to 46 µm and certain amount of FeB phase. The borides layer have poly phase (FeB/Fe_2B) and thickness of FeB phase increased with growing of

borides layer. The thickness of FeB was lower than half of total thickness of borides layer for the sample borided at 950° C for 5h. The higher boronizing temperature and duration, the higher FeB ratio to Fe_2B in the layer was observed. It was possibly reason of the fixing EMI-SE of around 75 dB.

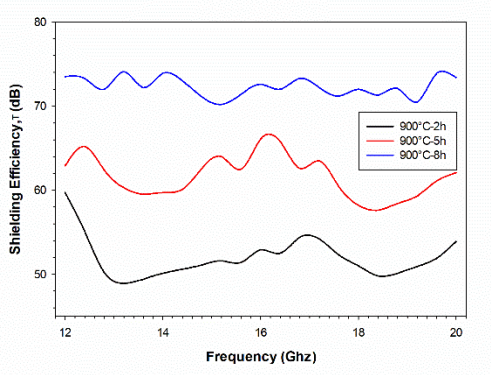

a)

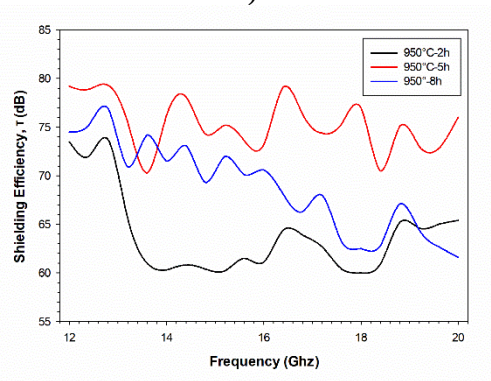

b)

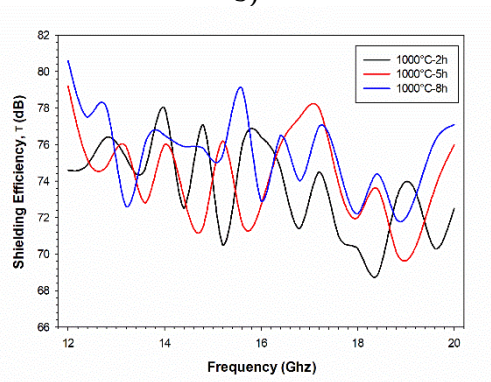

c)

Figure 6 Total EMI-SE in the Ku band of steel samples borided at a) 900°C, b) 950°C, c) 1000°C.

On the other hand, increasing FeB ratio and layer thickness led to narrower and more stable EMI-SE for samples borided at higher temperatures and durations (Fig.7).

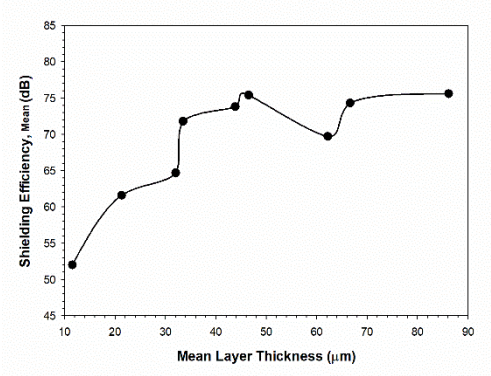

Figure 7 Variation of mean EMI-SE with borided layer thickness

4. CONCLUSIONS

The following results can be derived from this study,

a. The microstructure of borides formed on the surface of Mirrax steel was smooth morphology.
b. The thickness of borides layer, microhardness and penetration of microhardness were increased by increment of boriding temperature and time.
c. XRD revealed that borides layer showed biphasic nature (FeB, Fe_2B).
d. Maximum EMI-SE, total values increased from 50 to 80 dB as boriding time and temperature raised.
e. Mean EMI-SE of samples was increased with certain layer thickness (46 μm) and FeB ratio in the layer and it was found to be maximum 75 dB for sample borided at 950 °C for 5h.
f. It can be expressed that optimum EMI-SE values obtained in sample borided at 950 °C for 5h.
g. Layer thickness was more dominant effect than type of borides on the EMI-SE values. But, by increasing layer thickness and FeB amount made EMI-SE more stable within Ku band range.

ACKNOWLEDGEMENT

I would like to express my deepest thank to Prof. Dr. Cuma Bindal of Sakarya University for his invaluable supports.

REFERENCES

[1] N. Maruthi, M. Faisal and N. Raghavendra, "Conducting polymer based composites as efficient EMI shielding materials: A comprehensive review and future prospects," Synthetic Metals, vol. 272, pp. 1-20, 2021.

[2] G-H. Lim, N. Kwon, E. Han, S. Bok and S-E. Lee S, "Flexible Nanoporous Silver Membranes with Unprecedented High Effectiveness for Electromagnetic Interference Shielding," Journal of Industrial and Engineering Chemistry, Article in press, 2020.

[3] H. Liu, S. Wou, C. You, N. Tian, Y. Li and N. Chopra, "Recent progress in morphological engineering of carbon materials for electromagnetic interference shielding," Carbon, vol. 172, pp. 569–596, 2021.

[4] H. Zhang, B. Zhao, F-Z. Dai, H. Xiang and Z. Zhang, "$(Cr_{0.2}Mn_{0.2}Fe_{0.2}Co_{0.2}Mo_{0.2})B$: A novel high-entropy monoboride withgood electromagnetic interference shielding performance in K-band," Journal of Materials Science & Technology, vol. 77, pp. 58-65, 2021.

[5] N. L. Perrusquia, M. A. Doñu Ruiz, C.R. Torres San Miguel, G.J. Pérez Mendoza, J.V. Cortes Suarez and A. Juanico Loran, "Evaluation of properties in steel with boride coatings under hydrogen," Surface & Coatings Technology, vol. 377, pp. 1-9, 2019.

[6] G. K. Sireli, A. S. Bora and S. Timur, "Evaluating the mechanical behavior of electrochemically borided low carbon steel," Surface & Coatings Technology, vol. 381, pp. 1-10, 2020.

[7] M. Prince, S.L. Arjun, G. Surya Raj and P. Gopalakrishnan, "Experimental Investigations on the Effects of Multicomponent Laser Boriding on steels," Materials Today: Proceedings, vol. 5, pp. 25276-25284, 2018.

[8] S. A. Rosas-Meléndez, M. Elías-Espinosa, J.A. Reyes-Retana and F. Cervantes-Sodi, "Friction and wear of borided AISI O1 steel with carbon nanomaterial deposit," Materials Letters, vol. 282, pp. 1-4, 2021.

[9] A. Erdoğan, "Investigation of high temperature dry sliding behavior of borided H13 hot work tool steel with nanoboron powder," Surface & Coatings Technology, vol. 357, pp. 886-895, 2019.

[10] A. P. Krelling, C. E. da Costa, J.C.G. Milan and E.A.S. Almeida, "Micro-abrasive wear mechanisms of borided AISI 1020 steel," vol. 111, pp. 234-242, 2017.

[11] I. Turkmen, E. Yalamac and M. Keddam, "Investigation of tribological behaviour and diffusion model of Fe_2B layer formed by pack-boriding on SAE 1020 steel," Surface & Coatings Technology", vol. 377, pp. 1-12, 2019.

[12] I. Türkmen and E. Yalamaç, "Growth of the Fe2B layer on SAE 1020 steel employed a boron source of H3BO3 during the powder-pack boriding method," Journal of Alloys and Compounds, vol. 744, pp. 658-666, 2018.

[13] A. Bendoumi, N. Makuch, R. Chegroune, M. Kulka, M. Keddam, P. Dziarski and D. Przestacki, "The effect of temperature distribution and cooling rate on microstructure and microhardness of laser re-melted and laser-borided carbon steels with various carbon concentrations," Surface & Coatings Technology, vol. 387, pp. 1-20, 2020.

[14] E. H. Sanchez and J. C. Valezquez, "Kinetics of Growth of Iron Boride Layers on a Low-Carbon Steel Surface," Laboratory Unit Operations and Experimental Methods in Chemical Engineering-Chapter 3, pp. 37-55, IntechOpen, 2018.

[15] İ. Güneş, "Investigation of Tribological Properties and Characterization of Borided AISI 420 and AISI 5120 Steels," Trans Indian Inst Met, vol. 67, no. 3, pp. 359-365, 2014.

[16] N. Barut, D. Yavuz and Y. Kayalı, "Borlanmış AISI 5140 ve AISI 420 Çeliklerinin Difüzyon ve Adhezyon Davranışlarının İncelenmesi," Afyon Kocatepe Üniversitesi Fen ve Mühendislik Bilimleri Dergisi, vol. 14, pp. 1-8, 2014.

[17] P. Juijerm, "Diffusion kinetics of different boronizing processes on martensitic stainless steel AISI 420," Kovove Mater., vol. 52, pp. 232-236, 2014.

[18] C. Martini, G. Palombarini and M. Carbucicchio," Mechanism of thermochemical growth of iron borides on iron," Journal of Materials Science, vol. 39, pp. 933-937, 2004.

[19] Y. Kayali, "Investigation of the diffusion kinetics of borided stainless steels," Physics of Metals and Metallography, vol. 114, pp. 161-168, 2013.

[20] https://www.uddeholm.com/app/uploads/sites/40/2017/11/mirrax esr-eng p.1506-1602.pdf, Erişim tarihi: 12.01.2021.

[21] C. J. Scheuera, R. A. Fraga, R. P. Cardoso and S.F. Brunatto, "Effects Of Heat Treatment Condıtıons On Mıcrostructure And Mechanıcal Propertıes Of AISI 420 Steel," 21º CBECIMAT - Congresso Brasileiro de Engenharia e Ciência dos Materiais, pp. 5857-5867, 2014.